PCCP

PAPER

View Article Online
View Journal | View Issue

Cite this: *Phys. Chem. Chem. Phys.*, 2016, **18**, 12299

Effects of carbon vacancies on the structures, mechanical properties, and chemical bonding of zirconium carbides: a first-principles study†

Congwei Xie,*[ab] Artem R. Oganov,*[acde] Duan Li,[ab] Tekalign Terfa Debela,[ab] Ning Liu,[ab] Dong Dong[ab] and Qingfeng Zeng[ab]

Received 14th December 2015,
Accepted 30th March 2016

DOI: 10.1039/c5cp07724a

www.rsc.org/pccp

Interstitial carbides are able to maintain structural stability even with a high concentration of carbon vacancies. This feature provides them with tunable properties through the design of carbon vacancies, and thus making it important to reveal how carbon vacancies affect their properties. In the present study, using first-principles, we have calculated the properties of a number of stable and metastable zirconium carbides ZrC_{1-x} (x = 0 and 1/n, n = 2–8) which were predicted by the evolutionary algorithm USPEX. Effects of carbon vacancies on the structures, mechanical properties, and chemical bonding of these zirconium carbides were systematically investigated. The distribution of carbon vacancies has significant influence on mechanical properties, especially Pugh's ratio. Nonadjacent carbon vacancies enhance Pugh's ratio, while grouped carbon vacancies decrease Pugh's ratio. This is explained by the changes in strength of Zr–C and Zr–Zr bonding around differently distributed carbon vacancies. We further explored the mechanical properties of zirconium carbides with impurities (N and O) by inserting N and O atoms into the sites of carbon vacancies. The enhanced mechanical properties of zirconium carbides were found.

1 Introduction

Carbon atoms tend to locate at octahedral interstices in a close-packed transition metal lattice when the ratio of the atomic radius of carbon R_C to that of metal R_M satisfies the condition $0.41 < R_C/R_M < 0.59$.[1] Corresponding to this rule, carbides formed by carbon and group 4, 5, and 6 transition metals (without chromium) are described as interstitial compounds.[2] These interstitial carbides are also referred to as non-stoichiometric compounds provided that not all octahedral interstices are occupied by carbon atoms;[3] the unoccupied octahedral interstices are called carbon vacancies. It should be noted that non-stoichiometric interstitial carbides can maintain structural stability even if they accommodate abundant carbon vacancies.[4–7] Moreover, due to the existence of carbon vacancies, they generally display different properties as compared to their stoichiometric counterparts.[8,9] These unique characteristics provide us the possibility of tailoring the properties of interstitial carbides through the design of carbon vacancies, and thus making it important to study the effects of carbon vacancies on the properties of interstitial carbides.[10] Herein, taking zirconium carbide (a representative interstitial compound) as an example, we investigated how carbon vacancies affect properties.

Zirconium carbide is known as an outstanding high-temperature material. It has a broad range of technological applications because of its high hardness, extremely high melting point, good wear and corrosion resistance, and excellent high temperature thermal/mechanical properties.[9,11,12] In particular, it has great potential to be used as a nuclear fuel material due to its excellent resistance to fission product attack, low neutron cross-section, and considerable thermal conductivity.[11] Zirconium carbide has a rock-salt crystal structure with carbon atoms occupying the octahedral interstices of the *fcc* lattice constructed by zirconium atoms. Generally, carbon vacancies are easily formed in zirconium carbide and result in changes in

[a] *International Center for Materials Discovery, School of Materials Science and Engineering, Northwestern Polytechnical University, Xi'an, Shaanxi 710072, P. R. China. E-mail: xiecw1021@mail.nwpu.edu.cn*
[b] *Science and Technology on Thermostructural Composite Materials Laboratory, School of Materials Science and Engineering, Northwestern Polytechnical University, Xi'an, Shaanxi 710072, P. R. China*
[c] *Skolkovo Institute of Science and Technology, 3 Nobel street, Skolkovo 143025, Russia*
[d] *Moscow Institute of Physics and Technology, 9 Institutskiy Lane, Dolgoprudny City, Moscow Region 141700, Russia*
[e] *Department of Geosciences and Center for Materials by Design, Stony Brook University, Stony Brook, New York 11794, USA. E-mail: artem.oganov@stonybrook.edu*

† Electronic supplementary information (ESI) available: Dynamical and mechanical stability of zirconium carbides. See DOI: 10.1039/c5cp07724a

Table 1 Stable non-stoichiometric zirconium carbides discovered by order-parameter functional (OPF), cluster expansion (CE), and evolutionary algorithm (EA) methods

Compounds	Zr_8C_7	Zr_7C_6	Zr_6C_5	Zr_4C_3	Zr_3C_2	Zr_2C
OPF[15]			$C2/m$		$C222_1$	$Fd\bar{3}m$
CE[16]	$P4_332$		$C2/m$	$C2/m$	$Fddd$	$Fd\bar{3}m$
EA[17]		$R\bar{3}$		$C2/c$	$C2/m$	$Fd\bar{3}m$

properties.[13,14] Many research studies have been carried out to investigate the properties of non-stoichiometric zirconium carbides with various concentrations of carbon vacancies.[11] However, the current knowledge of explicit relationships between carbon vacancies and properties remains insufficient. The key to achieve this goal is to clarify crystal structures of non-stoichiometric zirconium carbides since crystal structures are helpful in the understanding of both carbon vacancies and properties.

During the last three decades, theoretical methods have played an important role in determining crystal structures of non-stoichiometric zirconium carbides.[15–17] As listed in Table 1, with the help of the order-parameter functional (OPF[18]), cluster expansion (CE[19]), and evolutionary algorithm (EA[20,21]) methods for structure prediction, a number of promising structures have been reported.[15–17] Checking these published studies, we found that their conclusions were more or less inaccurate. For instance, using the EA method, Yu *et al.*[17] discovered a new stable compound Zr_7C_6 ($R\bar{3}$), but they missed $Fddd$-Zr_3C_2 (a stable compound found by using the CE method[16]). Therefore, a more careful calculation is desired for searching for stable non-stoichiometric zirconium carbides.

In the present study, like Yu *et al.*, we also used the EA method for discovering stable non-stoichiometric zirconium carbides. This is because many stable carbides predicted by using the EA method have been experimentally confirmed (*e.g.*, in systems Ca–C,[22] Re–C,[23] and Tc–C[24]). We found that Zr_7C_6 ($R\bar{3}$), Zr_4C_3 ($C2/c$), Zr_3C_2 ($Fddd$), and Zr_2C ($Fd\bar{3}m$) are thermodynamically stable at 0 K and 0 GPa. Three metastable compounds ($P\bar{1}$-Zr_8C_7, $C2/m$-Zr_6C_5, and $P\bar{1}$-Zr_5C_4), with formation enthalpies a little above the thermodynamic convex hull, have also been discovered. They can be considered as nearly ground state compounds and are helpful in understanding the properties of non-stoichiometric zirconium carbides. We compared the present predicted structures with those suggested by previous calculations,[15–17] and found that the present prediction is more accurate. Based on the predicted stable and metastable structures, we investigated the effects of carbon vacancies on the structures, mechanical properties, and chemical bonding of zirconium carbides. Taking into account that interstitial carbides are prone to oxygen and nitrogen contamination during practical application,[11] we further investigated the effects of oxygen and nitrogen impurities on the mechanical properties of non-stoichiometric zirconium carbides by replacing carbon vacancies with oxygen and nitrogen atoms. Our present study would be helpful in understanding the properties of interstitial carbides with carbon vacancies or oxygen (nitrogen) impurities.

We organize the rest of the paper as follows: computational methods are presented in Section 2, main results are presented and discussed in Section 3, and conclusions are given in Section 4.

2 Computational methodology

The state-of-the-art EA method for structure prediction, performing global search and implemented in the USPEX code,[20,21] is used to predict stable non-stoichiometric zirconium carbides at 0 K and 0 GPa. The stability of a structure is determined using the thermodynamic convex hull construction. For every candidate structure generated by USPEX, total energy calculations and structure relaxations were carried out using density functional theory (DFT[25]) within the Perdew–Burke–Ernzerhof generalized gradient approximation (GGA[26]), as implemented in the VASP code.[27] In these calculations we used the all-electron projector-augmented wave method,[28] a plane-wave kinetic energy cutoff of 560 eV, and uniform k-point meshes with a reciprocal-space resolution of $2\pi \times 0.06$ Å^{-1}. These settings enable excellent convergence of energy differences, stress tensors, and structural parameters. Denser k-point meshes with a resolution of $2\pi \times 0.03$ Å^{-1} were used for detailed calculations of properties.

To check the dynamical stability of the predicted structures, a finite displacement method, as implemented in the PHONOPY code,[29,30] was used to obtain phonon dispersion curves. A structure is dynamically stable when no imaginary phonon frequencies have been found throughout the Brillouin zone. The elastic constants, directly related to the mechanical stability of a structure, were also calculated by VASP. For a mechanically stable structure with a given symmetry, its elastic constants should satisfy the corresponding stability criteria.[31] The mechanical properties (bulk modulus B and shear modulus G) of a material were evaluated using the Hill averaging scheme.[32,33] With B and G, the Vickers hardness H_V of a material can be obtained according to the Chen-Niu empirical model:[34]

$$H_V = 2(\kappa^2 G)^{0.585} - 3 \quad (1)$$

where κ (equals to G/B) is the Pugh's ratio,[35] and all moduli are in GPa. In most cases, the Chen-Niu model can evaluate very accurate Vickers hardness for a given material.

To relate mechanical properties with chemical bonding, we have computed the electronic density of states (DOS) and crystal orbital Hamiltonian populations (COHP) using VASP and LOBSTER programs,[36,37] respectively.

3 Results and discussion

3.1 Crystal structure prediction and structural properties

To search for stable non-stoichiometric zirconium carbides, we have performed an accurate EA prediction using the USPEX code for the Zr–ZrC system at 0 K and 0 GPa. The ground states of Zr ($P6_3/mmc$) and stoichiometric ZrC ($Fm\bar{3}m$) were chosen to construct the thermodynamic convex hull. As shown in Fig. 1, we have identified four stable non-stoichiometric compounds Zr_7C_6 ($R\bar{3}$), Zr_4C_3 ($C2/c$), Zr_3C_2 ($Fddd$), and Zr_2C ($Fd\bar{3}m$). In comparison to

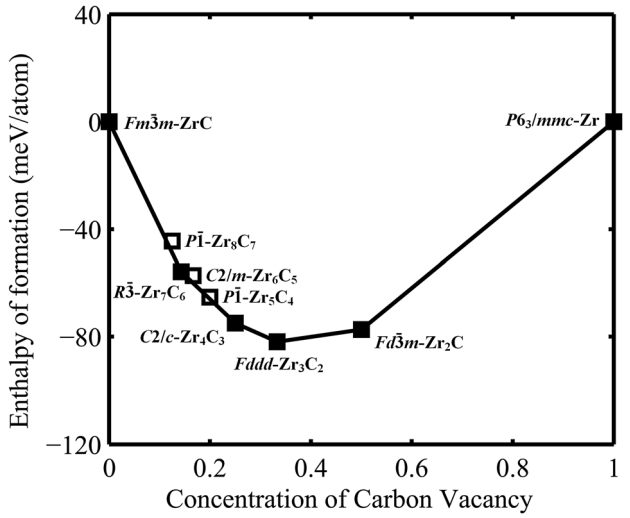

Fig. 1 Thermodynamic convex hull of the Zr–ZrC system. Solid squares denote stable compounds; open squares metastable compounds.

previous EA prediction performed by Yu *et al.*,[17] the present study has predicted the same structures for Zr_7C_6, Zr_4C_3, and Zr_2C, while a different structure *Fddd*-Zr_3C_2 instead of *C*2/*m*-Zr_3C_2. With the help of the CE method, Zhang *et al.*[16] discovered *Fddd*-Zr_3C_2, and they found that *Fddd*-Zr_3C_2 has lower energy than *C*2/*m*-Zr_3C_2. Here, we confirmed that *Fddd*-Zr_3C_2 is the ground state structure of Zr_3C_2. Yu *et al.* did not discover this structure using the EA method. That might be because they didn't perform sufficient configuration searching for Zr_3C_2. In the present EA prediction, we have also discovered three meta-stable non-stoichiometric zirconium carbides *P*$\bar{1}$-Zr_8C_7, *C*2/*m*-Zr_6C_5, and *P*$\bar{1}$-Zr_5C_4 (as shown in Fig. 1). The three meta-stable zirconium carbides were found to have formation enthalpies a little above the thermodynamic convex hull and thus can be considered as near-ground-state compounds. Among the three predicted meta-stable structures, *C*2/*m*-Zr_6C_5 has been reported before,[15] *P*$\bar{1}$-Zr_8C_7 and *P*$\bar{1}$-Zr_5C_4 were newly predicted and we have verified their dynamical and mechanical stability by computing phonon dispersion curves (see Fig. S1 & S2, ESI†) and elastic constants (see Table S1, ESI†). As discussed in the following section, the three metastable structures were also helpful in understanding the properties of zirconium carbides. Detailed structural information for these stable and meta-stable zirconium carbides is listed in Table 2.

Crystal structures of zirconium carbides are helpful in the understanding of carbon vacancies. In all the stable and

Table 2 Geometric details of the predicted stable and metastable zirconium carbides

Compounds	Lattice parameters (Å)	Wyckoff position	Coordination number
ZrC (*Fm*$\bar{3}$*m*)	a = 4.689	C(4b)(0.5000 0.5000 0.5000)	6
		Zr(4a)(0.0000 0.0000 0.0000)	6
Zr_8C_7 (*P*$\bar{1}$)	a = 5.789	C(2i)(0.2536 0.4976 0.1251)	6
	b = 9.961	C(2i)(0.2488 0.4948 0.6235)	6
	c = 6.634	C(2i)(0.0008 0.9996 0.7476)	6
	β = 125.17°	C(1d)(0.5000 0.0000 0.0000)	6
		Zr(2i)(0.8706 0.2454 0.0608)	6
		Zr(2i)(0.8929 0.2555 0.5653)	5
		Zr(2i)(0.3706 0.2550 0.8234)	5
		Zr(2i)(0.3725 0.2624 0.3062)	5
Zr_7C_6 (*R*$\bar{3}$)	a = 8.8404	C(18f)(0.5740 0.8599 0.0005)	6
	c = 8.2207	Zr(3b)(0.0000 0.0000 0.5000)	6
		Zr(18f)(0.7547 0.7998 0.1745)	5
Zr_6C_5 (*C*2/*m*)	a = 5.754	C(4h)(0.5000 0.3340 0.5000)	6
	b = 9.961	C(4g)(0.5000 0.3317 0.0000)	6
	c = 6.634	C(2b)(0.5000 0.0000 0.0000)	6
	β = 125.17°	Zr(8i)(0.4954 0.8268 0.7539)	5
		Zr(4i)(0.9792 0.0000 0.2393)	5
Zr_5C_4 (*P*$\bar{1}$)	a = 7.487	C(2i)(0.7994 0.3482 0.0983)	6
	b = 6.684	C(2i)(0.3995 0.5501 0.3020)	6
	c = 5.790	C(2i)(0.6038 0.9507 0.6996)	6
	α = 106.78°	C(2i)(0.0015 0.7523 0.4965)	6
	β = 75.07°	Zr(2i)(0.3026 0.3559 0.5873)	5
	γ = 102.84°	Zr(2i)(0.3057 0.8402 0.5906)	5
		Zr(2i)(0.5127 0.2560 0.0039)	5
		Zr(2i)(0.9074 0.5424 0.7940)	5
		Zr(2i)(0.1081 0.9501 0.2140)	4
Zr_4C_3 (*C*2/*c*)	a = 6.6783	C(4e)(0.0000 0.1849 0.7500)	6
	b = 13.3973	C(4e)(0.0000 0.9380 0.7500)	6
	c = 5.7971	C(4e)(0.0000 0.6868 0.7500)	6
	β = 125.20°	Zr(8f)(0.2432 0.1923 0.2492)	5
		Zr(8f)(0.2356 0.0668 0.7292)	4
Zr_3C_2 (*Fddd*)	a = 6.6724	C(16g)(0.5000 0.0000 0.4172)	6
	b = 9.4812	C(16g)(0.5000 0.0000 0.2500)	6
	c = 20.0598	Zr(32h)(0.4929 0.2587 0.0802)	4
		Zr(16e)(0.2394 0.0000 0.0000)	4
Zr_2C (*Fd*$\bar{3}$*m*)	a = 9.369	C(16d)(0.1250 0.12550 0.6250)	6
		Zr(32e)(0.3809 0.6191 0.6191)	3

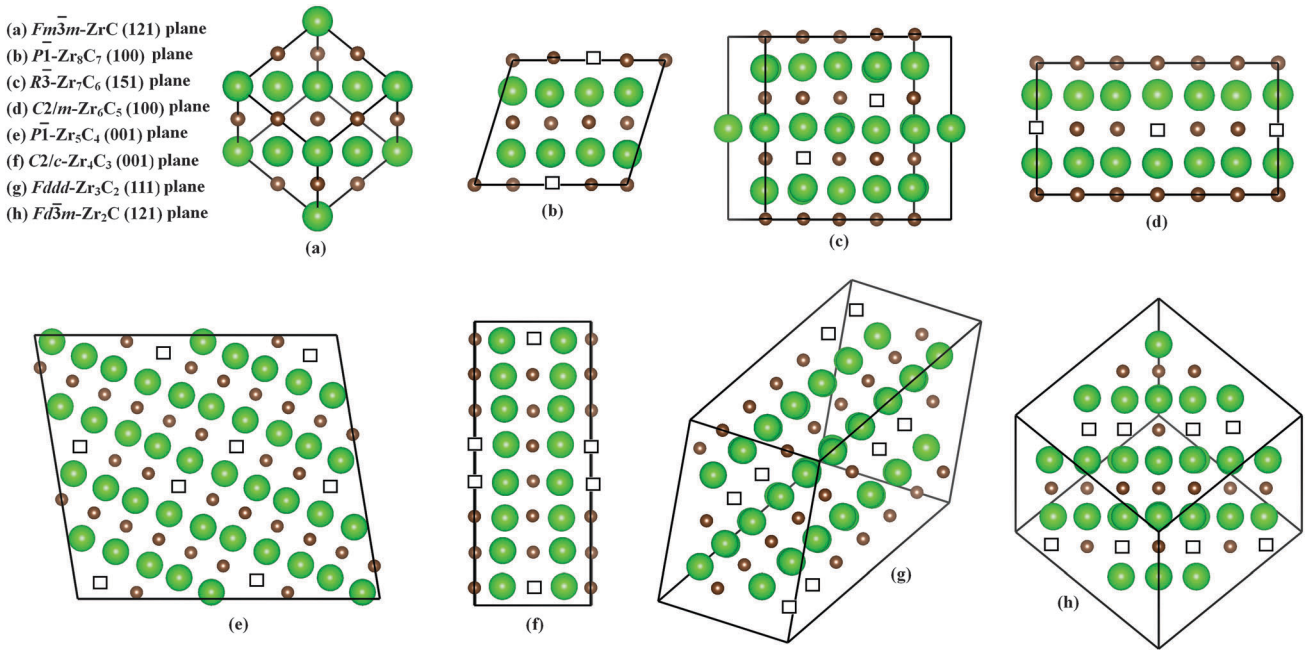

Fig. 2 (a–h) Atomic arrangement in the predicted stable and metastable zirconium carbides. Green spheres denote Zr atoms; brown spheres, C atoms; squares, carbon vacancies.

meta-stable zirconium carbides, carbon atoms occupy octahedral interstices in the cubic close packing of zirconium atoms, and carbon atoms are six-coordinate. In stoichiometric zirconium carbide ($Fm\bar{3}m$-ZrC), zirconium atoms are six-coordinated, while in non-stoichiometric zirconium carbides their coordination numbers are changed due to carbon vacancies (see Table 2). Coordination numbers of zirconium atoms can be used as indicators of the distribution of carbon vacancies: if the coordination numbers of zirconium atoms are not less than five, carbon vacancies are nonadjacent; if the coordination numbers of zirconium atoms are smaller than five, carbon vacancies are grouped. Fig. 2(a)–(h) show the distribution of carbon vacancies in a series of zirconium carbides as visualized using the VESTA software.[38] There are no carbon vacancies in the case of stoichiometric $Fm\bar{3}m$-ZrC. Carbon vacancies in non-stoichiometric $P\bar{1}$-Zr_8C_7, $R\bar{3}$-Zr_7C_6, and $C2/m$-Zr_6C_5 are nonadjacent. It should be noted that Zr_6C_5 is the composition with the maximum concentration of nonadjacent carbon vacancies when zirconium atoms are all five-coordinated. If the concentration of carbon vacancies continues to increase, the coordination numbers of zirconium atoms become smaller and smaller, and thus more and more carbon vacancies get grouped. As shown in Fig. 2(e)–(h), $P\bar{1}$-Zr_5C_4 possesses paired adjacent carbon vacancies, and carbon vacancies are interconnected in $C2/c$-Zr_4C_3, $Fddd$-Zr_3C_2, and $Fd\bar{3}m$-Zr_2C.

Like the concentration of carbon vacancies, the disturbution of carbon vacancies is also believed to have a great effect on the properties of interstitial carbides.[11] In the following sections, we will show how the concentration and distribution of carbon vacancies affect the mechanical and electronic properties of zirconium carbides.

Table 3 Calculated bulk modulus B (GPa), shear modulus G (GPa), Pugh's ratio κ ($\kappa = G/B$), and Vickers hardness H_V (GPa) of the predicted stable and metastable zirconium carbides at 0 GPa and 0 K

Properties	ZrC	Zr_8C_7	Zr_7C_6	Zr_6C_5	Zr_5C_4	Zr_4C_3	Zr_3C_2	Zr_2C
B	234 225[39] 223[40]	204	197	196	188	176	162	137
G	164 165[39] 170[40]	148	145	144	136	124	108	71
κ	0.701	0.724	0.736	0.734	0.726	0.705	0.667	0.523
H_V	23.4 23.0[39] 25.6[41]	22.5	22.7	22.5	21.4	19.3	16.3	8.4

3.2 Mechanical properties of zirconium carbides

The computed mechanical properties (bulk modulus B, shear modulus G, Pugh's ratio κ, and Vickers hardness H_V) of all the stable and meta-stable zirconium carbides are listed in Table 3. Our calculated results for the stoichiometric ZrC ($Fm\bar{3}m$) are in good agreement with the experimentally reported values,[39–41] supporting the accuracy and reliability for other non-stoichiometric compounds. As listed in Table 3, carbon vacancies are harmful to B, G, and H_V of zirconium carbides. However, we should note that non-stoichiometric zirconium carbides with low concentration of carbon vacancies still have high mechanical strength due to their high B, G, and H_V, while an obvious drop in mechanical strength can be found in those with a high concentration of carbon vacancies (*e.g.*, $Fddd$-Zr_3C_2 and $Fd\bar{3}m$-Zr_2C). Pugh's ratio κ is used as an indicator of mechanical brittleness; generally, a material is brittle if its κ is larger than 0.57.[35] It is found that κ varies with the

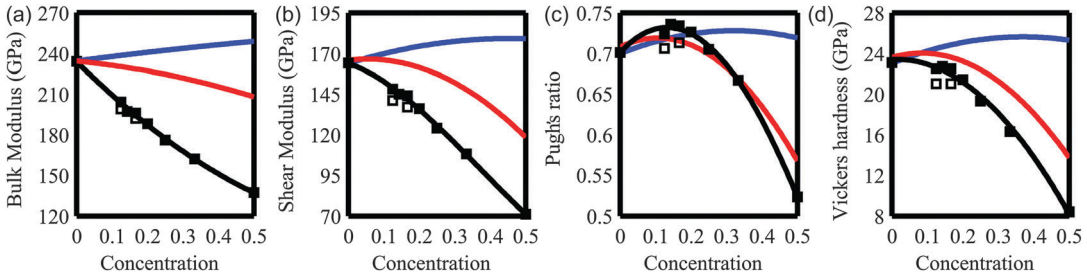

Fig. 3 Effects of carbon vacancies and impurities on the mechanical properties (bulk modulus, shear modulus, Pugh's ratio, and Vickers hardness) of the predicted stable and metastable zirconium carbides. Solid squares denote the predicted structures; open squares, constructed Zr_8C_7 and Zr_6C_5 structures with grouped carbon vacancies; black curves, the fitted curves for the concentration of carbon vacancies to mechanical properties; blue curves, the fitted curves for the concentration of nitrogen to mechanical properties; red curves, the fitted curves for the concentration of oxygen to mechanical properties.

concentration of carbon vacancies, suggesting that carbon vacancies can affect the brittleness of zirconium carbides. In particular, unlike other zirconium carbides, $Fd\bar{3}m$-Zr_2C is not a brittle material as indicated by its low κ (less than 0.57). This might be because of its high concentration of carbon vacancies; or in other words, high concentration of carbon vacancies may lead to brittle-to-non-brittle transformation. In fact, this explanation is understandable and reasonable if we consider the non-brittle pure zirconium as a "carbide" in which the concentration of carbon vacancies is 100%.

The relationships between the mechanical properties and the concentration of carbon vacancies are shown in Fig. 3 (denoted by solid squares and black curves). It seems that B and G vary linearly with the concentration of carbon vacancies, see Fig. 3(a) & (b). But this is not the case. For B and G, the dependence of at least one of them on the concentration of carbon vacancies should be nonlinear. Otherwise, with the increase of the concentration of carbon vacancies, κ (equals to G/B) must vary monotonically or should remain unchanged. The fact is that κ first increases and then decreases with increasing concentration of carbon vacancies, see Fig. 3(c). Therefore, we carefully analyzed the fitted curves for the concentration of carbon vacancies to B and G, and figured out the reason: (1) with the increase of the concentration of carbon vacancies, the B decreasing rate (dB/B) decreases, while the G decreasing rate (dG/G) increases; (2) at low concentration of carbon vacancies, dB/B is larger than dG/G; and (3) dB/B is equal to dG/G at a given concentration of carbon vacancies where the maximum κ occurs. A detailed mathematical analysis on the B (G) decreasing rate can be found in the ESI.† The dependence of H_V on the concentration of carbon vacancies is obviously nonlinear, see Fig. 3(d). At low concentration of carbon vacancies, H_V decreases very slowly, while at high concentration of carbon vacancies, H_V decreases quickly. The trend for hardness can be explained by κ (see eqn (1)).

We noticed that zirconium carbides with the concentration of carbon vacancies of around 1/6 may have the maximum κ, see Fig. 3(c). Surprisingly, this concentration of carbon vacancies indicates the forthcoming of grouped carbon vacancies. The coincidence hinted us to relate κ to the distribution of carbon vacancies. We suppose that nonadjacent carbon vacancies enhance κ, while grouped carbon vacancies decrease κ. In view of the relationship between κ and H_V, we can also suppose that nonadjacent carbon vacancies have a smaller contribution to the decrease of hardness than adjacent carbon vacancies. To check these hypotheses, we constructed two zirconium carbides with grouped carbon vacancies $P2/c$-Zr_8C_7 and $Fddd$-Zr_6C_5 (denoted by the open squares in Fig. 3) based on $C2/c$-Zr_4C_3 and $Fddd$-Zr_3C_2, respectively. In contrast to $P\bar{1}$-Zr_8C_7 with nonadjacent carbon vacancies, $P2/c$-Zr_8C_7 has lower κ and H_V. Similarly, κ and H_V of $Fddd$-Zr_6C_5 are lower than those of $C2/m$-Zr_6C_5 with nonadjacent vacancies. This confirms our hypothesis that the distribution of carbon vacancies has a great effect on the κ of zirconium carbides. And this hypothesis is supported by the following chemical bonding analysis of zirconium carbides.

3.3 Chemical bonding of zirconium carbides

Mechanical properties are often directly related to chemical bonding. To identify chemical boding in zirconium carbides, we have computed the electronic density of states (DOS) and the atom-resolved partial densities of states (PDOS) for all the stable and meta-stable zirconium carbides. As shown in Fig. 4, all these zirconium carbides have finite electronic DOS at the Fermi level which is mainly contributed by zirconium's d electrons. This feature indicates the existence of metallic Zr–Zr bonding in zirconium carbides. Below the Fermi level, strong hybridization of the d-orbital of Zr and the p-orbital of C atoms is observed, implying the strong covalency of Zr–C bonding. In the present study, we didn't mention the ionic character of Zr–C bonding due to its negligible effect on mechanical properties.[11]

The density and strength of chemical bonding are two important factors helpful in understanding the mechanical properties of zirconium carbides. In zirconium carbides, densities of Zr–Zr bonding are almost the same due to the negligible effect of carbon vacancies on volume (within 0.5%). By contrast, the density of Zr–C bonding decreases with the increase of the concentration of carbon vacancies. The bonding strength of Zr–Zr and Zr–C bonds in zirconium carbides was also investigated. In general, the integrated crystal orbital Hamiltonian population (ICOHP) value of a chemical bond is an indicator of its bonding strength.[37] By computing the crystal orbital Hamiltonian population (COHP), we have obtained the –ICOHP

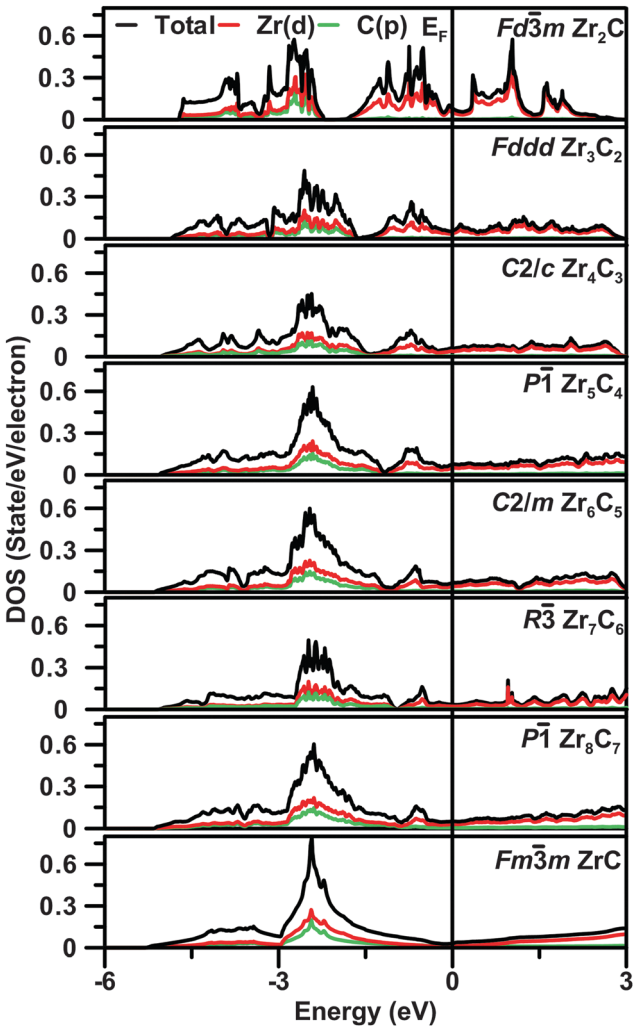

Fig. 4 The calculated density of states (DOS) for all the predicted stable and metastable zirconium carbides.

values for Zr–Zr and Zr–C bonds in all the stable and meta-stable zirconium carbides. As listed in Table 4, the averaged –ICOHP values of Zr–C bonding decrease with the increase of the concentration of carbon vacancies, indicating the weakening of Zr–C bonding. In contrast, Zr–Zr bonding strengthens with the increase of the concentration of carbon vacancies due to the increase of the averaged –ICOHP values of Zr–Zr bonding. Even so, in zirconium carbides, covalent Zr–C bonding is obvious to be much stronger than metallic Zr–Zr bonding as indicated by their averaged –ICOHP values. This makes us believe that strong covalent Zr–C bonding plays a dominant role in determining mechanical properties such as B and G of zirconium carbides. Thus, the loss in B and G of zirconium carbides can be ascribed to two main factors: (1) densities of Zr–C bonding are decreased; and (2) Zr–C bonding are weakened. The strengthened metallic bonding has long been believed to decrease G.[42] Thus, enhanced Zr–Zr bonding with the increase of the concentration of carbon vacancies is also possible to lead to the decrease of G.

Unlike B and G, κ firstly increases and then decreases with the increase of the concentration of carbon vacancies. As discussed in Section 3.2, we suggested that the trend for κ is related to the distribution of carbon vacancies. Here, we further tried to explain this view using chemical bonding analysis. It has been reported that chemical bonding strength has impact on κ.[43,44] The stronger the covalent bonding (or the weaker the metallic bonding), the higher the κ. We investigated the effects of the distribution of carbon vacancies on the strength of chemical bonding. In order to analyze easily, we used Zr(i) to denote i-coordinate Zr atoms (i = 6, 5, 4, 3), where i = 6 represents no vacancies, i = 5 nonadjacent vacancies, and i = 4 or 3 grouped vacancies. A general map of –ICOHP values and lengths of Zr(i)–C and Zr(i)–Zr bonds in all the stable zirconium carbides is shown in Fig. 5. From Fig. 5, we can find that those strongest Zr–C bonds are formed by 5-coordinate Zr atoms. Meanwhile, Zr(5)–Zr bonds are still weak due to their small -ICOHP values (less than 0.43 eV per atom[45]). That means nonadjacent vacancies can act as local strengthening centers and thus may explain the increase of κ. In the case of 4- and 3-coordinate Zr atoms, the strongest Zr–Zr bonds are found to have –ICOHP values around 0.8 eV per bond (similar to 0.75 eV per bond found in $Fm\bar{3}m$ Zr in this study), indicating that Zr–Zr bonds around adjacent vacancies are strong. At the same time, Zr(4)– and Zr(3)–C bonds become weaker than Zr(5)–C bonds. Thus, κ in zirconium carbides with grouped vacancies decreases. By analogy with κ, trends for hardness can be explained as well (see eqn (1)).

3.4 Mechanical properties of zirconium carbides with impurities

In practical applications, carbon vacancy sites are easily occupied by some other elements, and thus the properties of zirconium carbides could be altered.[46,47] Herein, taking into account that interstitial carbides are prone to oxygen and nitrogen contamination,[11] we investigated the effects of oxygen (nitrogen) impurities on the mechanical properties of zirconium carbides. In principle, we need to perform a global search for these ternary systems, which would require calculations for many compositions and, for each composition, many configurations. However, this is very time-consuming and our purpose is not to study all possible compositions and their lowest-energy configurations. We aim at providing some information by studying some possible compositions and configurations.

Table 4 The averaged integrated crystal orbital Hamiltonian population (–ICOHP) values (in eV per bond) computed for Zr–C and Zr–Zr bonds in all the predicted stable and metastable zirconium carbides

Chemical bonding	ZrC	Zr_8C_7	Zr_7C_6	Zr_6C_5	Zr_5C_4	Zr_4C_3	Zr_3C_2	Zr_2C
Zr–C	1.47 ± 0	1.45 ± 0.12	1.45 ± 0.14	1.44 ± 0.12	1.43 ± 0.12	1.42 ± 0.10	1.38 ± 0.07	1.29 ± 0
Zr–Zr	0.14 ± 0	0.21 ± 0.11	0.22 ± 0.11	0.25 ± 0.12	0.26 ± 0.14	0.30 ± 0.16	0.35 ± 0.17	0.46 ± 0.21

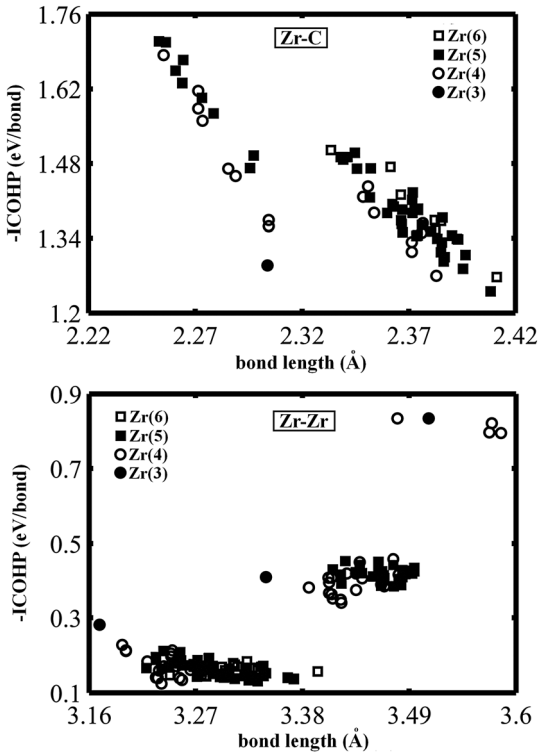

Fig. 5 The integrated crystal orbital Hamiltonian population (–ICOHP) values (in eV per bond) and bond lengths (in Å) of Zr(i)–C and Zr(i)–Zr bonds, where i denotes the Zr coordination number.

Table 5 The calculated formation enthalpies ΔH (eV per atom) for $ZrC_{1-x}T_x$ (T = N and O; x = 1/8, 1/7, 1/6, 1/5, 1/4, 1/3 and 1/2) compounds, defined as $\Delta H(ZrC_{1-x}T_x) = (E(ZrC_{1-x}T_x) - E(ZrC_{1-x}) - xE(T))/2$

T	Zr_8C_7T	Zr_7C_6T	Zr_6C_5T	Zr_5C_4T	Zr_4C_3T	Zr_3C_2T	Zr_2CT
N	−0.189	−0.213	−0.260	−0.314	−0.399	−0.547	−0.855
O	−0.329	−0.372	−0.438	−0.523	−0.658	−0.874	−1.309

Based on the predicted stable and metastable non-stoichiometric zirconium carbides Zr_8C_7 ($P\bar{1}$), Zr_7C_6 ($R\bar{3}$), Zr_6C_5 ($C2/m$), Zr_5C_4 ($P\bar{1}$), Zr_4C_3 ($C2/c$), Zr_3C_2 ($Fddd$), and Zr_2C ($Fd\bar{3}m$), we constructed seven $ZrC_{1-x}T_x$ (x = 1/n, n = 2–8) structures for each element T (T = N and O) and calculated their mechanical properties. These structures are reasonable in terms of their negative formation enthalpies (see Table 5). The relationships between the mechanical properties of $ZrC_{1-x}T_x$ compounds and the T content are shown in Fig. 3 (N and O doping is denoted by blue and red curves, respectively). We found that N and O impurities can enhance the bulk modulus, shear modulus, and hardness of zirconium carbides.

4 Conclusions

In summary, evolutionary structure prediction using the USPEX code has been used to predict stable non-stoichiometric zirconium carbides. We have identified four stable non-stoichiometric compounds Zr_7C_6 ($R\bar{3}$), Zr_4C_3 ($C2/c$), Zr_3C_2 ($Fddd$), and Zr_2C ($Fd\bar{3}m$). Three meta-stable non-stoichiometric zirconium carbides $P\bar{1}$-Zr_8C_7, $C2/m$-Zr_6C_5, and $P\bar{1}$-Zr_5C_4, with formation enthalpies a little above the thermodynamic convex hull, were also been found. In contrast to the stoichiometric zirconium carbide ZrC ($Fm\bar{3}m$), all the predicted stable and metastable zirconium carbides have ordered carbon vacancies. We have investigated effects of carbon vacancies on the structural, mechanical, and electronic properties of zirconium carbides. When the concentration of carbon vacancies is not higher than 1/6, non-stoichiometric zirconium carbides prefer to adopt structures with nonadjacent vacancies. When the concentration of carbon vacancies is higher than 1/6, carbon vacancies are grouped in zirconium carbides. Such an evolution of the distribution of carbon vacancies can affect the mechanical properties of zirconium carbides, especially Pugh's ratio – an indicator of brittleness. We conclude that nonadjacent carbon vacancies enhance Pugh's ratio, while grouped carbon vacancies decrease Pugh's ratio. This conclusion is supported by chemical bonding analysis and explains why $Fd\bar{3}m$-Zr_2C is non-brittle. We further investigated the effects of impurities (N and O) on the mechanical properties of zirconium carbides by inserting N and O atoms into the carbon vacancy sites. The enhanced mechanical properties of zirconium carbides were found.

Acknowledgements

C. W. Xie thanks Dr H. Y. Niu for discussions. This work was supported by the Natural Science Foundation of China (Nos. 51372203 and 51332004), the Foreign Talents Introduction and Academic Exchange Program of China (No. B08040), and the Government of Russian Federation (Grant No. 14.A12.31.0003). The authors also acknowledge the High Performance Computing Center of NWPU for the allocation of computing time on their machines.

References

1 G. Hagg, *Z. Phys. Chem.*, 1931, **12**, 33–56.
2 N. N. Greenwood and A. Earnshaw, *Chemistry of the Elements*, Pergamon Press, Oxford, 1984.
3 A. Gusev, *Phys. Status Solidi B*, 1991, **163**, 17–54.
4 C. H. de Novion and J. P. Landesman, *Pure Appl. Chem.*, 1985, **57**, 1391–1402.
5 A. I. Gusev and A. A. Rempel, *Phys. Status Solidi A*, 1993, **135**, 15–58.
6 A. A. Rempel, *Phys.-Usp.*, 1996, **39**, 31.
7 A. I. Gusev, *Phys.-Usp.*, 2000, **43**, 1–37.
8 I. Pollini, A. Mosser and J. C. Parlebas, *Phys. Rep.*, 2001, **355**, 1–72.
9 H. O. Pierson, *Handbook of Refractory Carbides & Nitrides: Properties, Characteristics, Processing and Apps.*, William Andrew, 1996.
10 X.-X. Yu, G. B. Thompson and C. R. Weinberger, *J. Eur. Ceram. Soc.*, 2015, **35**, 95–103.
11 Y. Katoh, G. Vasudevamurthy, T. Nozawa and L. L. Snead, *J. Nucl. Mater.*, 2013, **441**, 718–742.

12 M. M. Opeka, I. G. Talmy, E. J. Wuchina, J. A. Zaykoski and S. J. Causey, *J. Eur. Ceram. Soc.*, 1999, **19**, 2405–2414.
13 W. Hu, J. Xiang, Y. Zhang, S. Liu, C. Chen, P. Wang, H. Wang, F. Wen, B. Xu, J. He, D. Yu, Y. Tian and Z. Liu, *J. Mater. Res.*, 2012, **27**, 1230–1236.
14 Y. Yang, W.-Y. Lo, C. Dickerson and T. R. Allen, *J. Nucl. Mater.*, 2014, **454**, 130–135.
15 A. I. Gusev and A. A. Rempel, *J. Phys. Chem. Solids*, 1994, **55**, 299–304.
16 Y. Zhang, B. Liu and J. Wang, *Sci. Rep.*, 2015, **5**, 18098.
17 X.-X. Yu, C. R. Weinberger and G. B. Thompson, *Comput. Mater. Sci.*, 2016, **112**, 318–326.
18 A. Gusev, *Philos. Mag. B*, 1989, **60**, 307–324.
19 J. W. D. Connolly and A. R. Williams, *Phys. Rev. B: Condens. Matter Mater. Phys.*, 1983, **27**, 5169–5172.
20 A. R. Oganov and C. W. Glass, *J. Chem. Phys.*, 2006, **124**, 244704.
21 C. W. Glass, A. R. Oganov and N. Hansen, *Comput. Phys. Commun.*, 2006, **175**, 713–720.
22 Y.-L. Li, S.-N. Wang, A. R. Oganov, H. Gou, J. S. Smith and T. A. Strobel, *Nat. Commun.*, 2015, **6**, 6974.
23 W. Sun, Y. Li, L. Zhu, Y. Ma, I. Di Marco, B. Johansson and P. Korzhavyi, *Phys. Chem. Chem. Phys.*, 2015, **17**, 9730–9736.
24 Q. Wang, K. E. German, A. R. Oganov, H. Dong, O. D. Feya, Y. V. Zubavichus and V. Y. Murzin, *RSC Adv.*, 2016, **6**, 16197–16202.
25 W. Kohn and L. J. Sham, *Phys. Rev.*, 1965, **140**, A1133.
26 J. P. Perdew, K. Burke and M. Ernzerhof, *Phys. Rev. Lett.*, 1996, **77**, 3865.
27 G. Kresse and J. Furthmüller, *Phys. Rev. B: Condens. Matter Mater. Phys.*, 1996, **54**, 11169–11186.
28 P. E. Blöchl, *Phys. Rev. B: Condens. Matter Mater. Phys.*, 1994, **50**, 17953.
29 D. Alfè, *Comput. Phys. Commun.*, 2009, **180**, 2622–2633.
30 A. Togo, F. Oba and I. Tanaka, *Phys. Rev. B: Condens. Matter Mater. Phys.*, 2008, **78**, 134106.
31 M. Born and K. Huang, *Dynamical theory of crystal lattices*, Oxford University Press, 1998.
32 R. Hill, *J. Mech. Phys. Solids*, 1963, **11**, 357–372.
33 R. Hill, *Proc. Phys. Soc., London, Sect. A*, 1952, **65**, 349.
34 X.-Q. Chen, H. Niu, D. Li and Y. Li, *Intermetallics*, 2011, **19**, 1275–1281.
35 S. Pugh, *London, Edinburgh Dublin Philos. Mag. J. Sci.*, 1954, **45**, 823–843.
36 V. L. Deringer, A. L. Tchougréeff and R. Dronskowski, *J. Phys. Chem. A*, 2011, **115**, 5461–5466.
37 S. Maintz, V. L. Deringer, A. L. Tchougréeff and R. Dronskowski, *J. Comput. Chem.*, 2013, **34**, 2557–2567.
38 K. Momma and F. Izumi, *J. Appl. Crystallogr.*, 2011, **44**, 1272–1276.
39 Q. Yang, W. Lengauer, T. Koch, M. Scheerer and I. Smid, *J. Alloys Compd.*, 2000, **309**, L5–L9.
40 R. Chang and L. J. Graham, *J. Appl. Phys.*, 1966, **37**, 3778–3783.
41 H. Holleck, *J. Vac. Sci. Technol., A*, 1986, **4**, 2661–2669.
42 S.-H. Jhi, S. G. Louie, M. L. Cohen and J. Morris Jr, *Phys. Rev. Lett.*, 2001, **87**, 075503.
43 Z. Liu, D. Gall and S. Khare, *Phys. Rev. B: Condens. Matter Mater. Phys.*, 2014, **90**, 134102.
44 D. Music, A. Houben, R. Dronskowski and J. M. Schneider, *Phys. Rev. B: Condens. Matter Mater. Phys.*, 2007, **75**, 174102.
45 C. Lee, A. Safa-Sefat, J. Greedan and H. Kleinke, *Chem. Mater.*, 2003, **15**, 780–786.
46 S.-H. Jhi, J. Ihm, S. G. Louie and M. L. Cohen, *Nature*, 1999, **399**, 132–134.
47 Y. Pipon, N. Toulhoat, N. Moncoffre, G. Gutierrez, A. Maitre and M. Gendre, *J. Nucl. Mater.*, 2013, **440**, 546–552.

